

Generation of an arbitrary four-photon polarization-entangled decoherence-free state with cross-Kerr nonlinearity

Meiyu Wang¹ · Fengli Yan¹ · Ting Gao²

Received: 3 March 2017 / Accepted: 15 June 2017 / Published online: 1 July 2017
© Springer Science+Business Media, LLC 2017

Abstract We present a new scheme to provide an arbitrary four-photon polarization-entangled state, which enables the encoding of single logical qubit information into a four-qubit decoherence-free subspace robustly against collective decoherence. With the assistance of the cross-Kerr nonlinearities, a spatial entanglement gate and a polarization entanglement gate are inserted into the circuit, where the X-quadrature homodyne measurement is properly performed. According to the outcomes of homodyne measurement in the spatial entanglement process, some swap gates are inserted into the corresponding paths of the photons to swap their spatial modes. Apart from Kerr media, some basic linear optical elements are necessary, which make it feasible with current experimental techniques.

Keywords Decoherence-free state · Cross-Kerr nonlinearity · X-quadrature homodyne measurement

✉ Fengli Yan
flyan@mail.hebtu.edu.cn

✉ Ting Gao
gaoting@mail.hebtu.edu.cn

Meiyu Wang
meiyu00_2001@163.com

¹ College of Physics Science and Information Engineering, Hebei Normal University, Shijiazhuang 050024, China

² College of Mathematics and Information Science, Hebei Normal University, Shijiazhuang 050024, China

1 Introduction

Entanglement [1–3] plays an important role in quantum information processing (QIP), such as long-distance quantum communication and distributed quantum computation. In order to complete these QIP protocols perfectly, maximally entangled states are usually required. However, in a realistic situation, decoherence, induced by uncontrolled coupling between a quantum system and the environment, is a significant obstacle to the realization of QIP. When qubits are coupled to the environment, the quantum superposition and coherence are easily destructed, and as a result, the maximally entangled state collapses into a nonmaximally entangled one or even a mixed state. This will degrade the fidelity and security of quantum communication. Since it is impossible to perfectly isolate a quantum system from its surrounding environment, decoherence effects are more or less inevitable. Overcoming the destructive effects of decoherence is the central issue for quantum communication and computation. Many strategies addressing this challenge have been focused on using either quantum error corrections [4, 5], dynamical decoupling [6, 7], entanglement concentration [8–11] or decoherence-free subspaces (DFSs) [12–15]. In these approaches, the proposal of DFSs is a promising way. Provided that the interaction between the system and the environment exhibits a certain symmetry, the particular subspaces of the overall Hilbert space are immune to the decoherence induced by this symmetrical interaction. That is, when the decoherence-free (DF) states are influenced by this symmetrical interaction, no matter how strong this qubit–environment interaction, they exhibit some symmetry, so the quantum states are invariant under this interaction. This property makes the decoherence-free states also useful for long-distance quantum information transmission and storage.

The N -qubit decoherence-free states were originally proposed by Kempe et al. [14]. For two qubits, there is only one decoherence-free singlet state, i.e., $\frac{1}{\sqrt{2}}(|01\rangle - |10\rangle)$. Therefore, it is not sufficient to fully protect the quantum information of an arbitrary logical qubit against collective noise. Another nontrivial example is the four-qubit entangled decoherence-free state

$$|\Phi_0\rangle = \alpha|0\rangle_L + \beta|1\rangle_L, \quad (1)$$

where

$$|0\rangle_L = \frac{1}{2}(|01\rangle - |10\rangle)(|01\rangle - |10\rangle), \quad (2)$$

$$|1\rangle_L = \frac{1}{2\sqrt{3}}(2|0011\rangle + 2|1100\rangle - |0101\rangle - |1010\rangle - |0110\rangle - |1001\rangle). \quad (3)$$

The dimension of the above four-qubit decoherence-free state in Eq. (1) is 2, and thus it is sufficient to fully protect an arbitrary logical qubit against collective noise in contrast to the two-qubit state. With its interesting applications, DFSs have been extensively studied both in theoretical and in experimental frames [16–20]. Bourennane et al. [16] did an experiment to generate four-photon polarization-entangled decoherence-free states via a spontaneous parametric down-conversion source. Subsequently, Zou

et al. [17] and Gong et al. [18] proposed two different schemes to generate four-photon polarization-entangled decoherence-free states based on linear optical elements and postselection strategy. In 2011, Wang et al. [19] proposed a probabilistic linear-optics-based scheme for local conversion of four Einstein–Podolsky–Rosen photon pairs into four-photon polarization-entangled decoherence-free states. Very recently, Zhou et al. [20] proposed three effective protocols to generate four-qubit entangled decoherence-free states assisted by the cavity-QED system.

In this paper, we present a new scheme to generate the four-photon polarization-entangled decoherence-free state with the help of the cross-Kerr nonlinearities. Due to the fact that photons have the merits of higher speed, lower decoherence, easier manipulation and lower energy cost compared with more massive qubits, we use the polarization of photons as qubit and define the horizontally (vertically) linear polarization $|H\rangle$ ($|V\rangle$) as the qubit $|0\rangle$ ($|1\rangle$). The photonic QIP requires interactions between photons. One possible coupling mechanism is the cross-Kerr nonlinearity, where the photons interact via a nonlinear medium. The cross-Kerr nonlinearity between photons offers an ideal playground for quantum state engineering, and a number of applications have been studied, such as constructing nondestructive quantum nondemolition detectors (QND) [21,22], quantum logic gates [22–24], deterministic entanglement distillation [25], logic-qubit entanglement [26,27], generation of multi-photon-entangled states and three- or four-photon decoherence-free states [28–33].

The paper is organized as follows. We begin by briefly reviewing the cross-Kerr nonlinearity, which was first used in Ref. [34], and describe the generation process of the four-photon polarization-entangled DF state with the assistance of weak cross-Kerr nonlinearities in Sect. 2. The discussion and conclusion are presented in Sect. 3.

2 Generation of four-qubit entangled decoherence-free states

The cross-Kerr nonlinearity can be described with the Hamiltonian $\hat{H}_k = -\hbar\kappa\hat{n}_s\hat{n}_p$, where \hat{n}_s (\hat{n}_p) is the photon number operator of the signal (probe) mode, and κ is the strength of the nonlinearity. If the signal field contains n photons and the probe field is in an initial coherent state with amplitude α , the cross-Kerr nonlinearity interaction causes the combined signal-probe system to evolve as follows:

$$e^{-i\hat{H}_k t/\hbar} |n\rangle_s |\alpha\rangle_p = e^{i\kappa t \hat{n}_s \hat{n}_p} |n\rangle_s |\alpha\rangle_p = |n\rangle_s |\alpha e^{in\theta}\rangle_p, \tag{4}$$

where $\theta = \kappa t$ with t being the interaction time. It is easy to observe that signal-photon state is unaffected by the interaction but the coherent state picks up a phase shift $n\theta$ directly proportional to the number of photons n in the signal mode. One can exactly obtain the information of photons in the signal state but cannot destroy them through a general homodyne–heterodyne measurement of the phase of the coherent state. This technique was first used to realize a parity gate [21] and then a CNOT gate [22], where the requirement for this technique is $\alpha\theta^2 > 9$ with α denoting the amplitude of the coherent state. As for the cross-Kerr nonlinearity, the nonlinearity magnitude $\theta \sim 10^{-2}$ is potentially available with the help of electromagnetically induced transparency [35]. In particular, the error probability is $P_{\text{error}} = 3.4 \times 10^{-6}$ on the condition

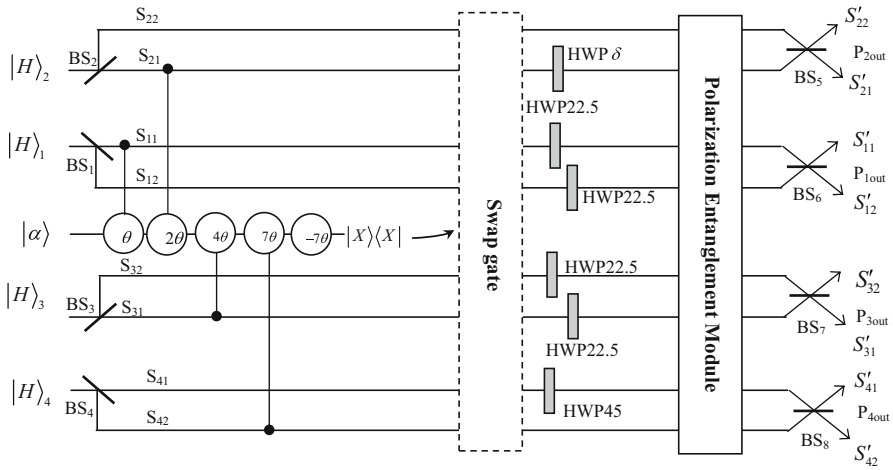


Fig. 1 Illustration plot for generating four-photon polarization-entangled decoherence-free state with the help of the cross-Kerr nonlinearities. The beam splitters BS₁, BS₂ and BS₃ have equal probability (50:50) of transmission and reflection, while BS₄ has the ratio $A_1^2 : A_2^2$ for the reflection and transmission coefficients. HWP22.5, HWP45 and HWP δ denote half-wave plates which realize the Hadamard transformation operation, single-photon σ_x operation and rotation of 2δ on the basis $\{|H\rangle, |V\rangle\}$, respectively. In the construction of the circuit, after a spatial entanglement module, the swap gates and the polarization entanglement module are need to be performed, which can be seen in Figs. 2 and 3, respectively. Before four photons leave the circuit, the eight potential paths of four photons are coherently combined by BS₅–BS₈ for obtaining the four-photon polarization-entangled decoherence-free state

$\alpha = 90000, \theta = 0.01$. This shows that it is still possible to operate in the regime of weak cross-Kerr nonlinearity, and the amplitude of the probe coherent state beam is physically reasonable with current experimental technology. Our scheme of preparing quantum-entangled state also works with the weak cross-Kerr nonlinearity.

In what follows, we explain the detailed procedures for generating the four-photon polarization-entangled decoherence-free state abided by the following processes, which is also illustrated in Fig. 1.

Assume the four single photons are initially prepared in the state $|H\rangle_1 \otimes |H\rangle_2 \otimes |H\rangle_3 \otimes |H\rangle_4$, and let them enter into the circuit shown in Fig. 1 from the input ports. In the spatial entanglement gate, four photons pass through beam splitters (BS₁, BS₂, BS₃ and BS₄). The BSs' reflectivity and transmissivity are independent of polarizations, and BSs have the following function between two input modes (a,b) and two output modes (c,d): $a^\dagger \rightarrow (A_1 c^\dagger + A_2 d^\dagger), b^\dagger \rightarrow (A_1 c^\dagger - A_2 d^\dagger)$, where the reflection and transmission coefficients of the BS₁, BS₂ and BS₃ are $A_1 = A_2 = \frac{1}{\sqrt{2}}$. Accompanying with a coherent state, the four photons enter into Kerr media; the evolution process of four photons interacting with the coherent state $|\alpha\rangle$ can be expressed as

$$\frac{1}{2\sqrt{2}}(|H\rangle_1|S_{11}\rangle + |H\rangle_1|S_{12}\rangle)(|H\rangle_2|S_{21}\rangle + |H\rangle_2|S_{22}\rangle)(|H\rangle_3|S_{31}\rangle + |H\rangle_3|S_{32}\rangle)(A_2|H\rangle_4|S_{41}\rangle + A_1|H\rangle_4|S_{42}\rangle)$$

$$\begin{aligned}
 \xrightarrow{\text{Kerr media}} & \frac{1}{2\sqrt{2}} |H\rangle_1 |H\rangle_2 |H\rangle_3 |H\rangle_4 [(A_2 |S_{11}\rangle |S_{21}\rangle |S_{31}\rangle |S_{41}\rangle \\
 & + A_1 |S_{12}\rangle |S_{22}\rangle |S_{32}\rangle |S_{42}\rangle) |\alpha\rangle \\
 & + (A_2 |S_{12}\rangle |S_{21}\rangle |S_{31}\rangle |S_{41}\rangle |\alpha e^{-i\theta}\rangle + A_1 |S_{11}\rangle |S_{22}\rangle |S_{32}\rangle |S_{42}\rangle |\alpha e^{i\theta}\rangle) \\
 & + (A_2 |S_{11}\rangle |S_{22}\rangle |S_{31}\rangle |S_{41}\rangle |\alpha e^{-i2\theta}\rangle + A_1 |S_{12}\rangle |S_{21}\rangle |S_{32}\rangle |S_{42}\rangle |\alpha e^{i2\theta}\rangle) \\
 & + (A_2 |S_{12}\rangle |S_{22}\rangle |S_{31}\rangle |S_{41}\rangle |\alpha e^{-i3\theta}\rangle + A_1 |S_{11}\rangle |S_{21}\rangle |S_{32}\rangle |S_{42}\rangle |\alpha e^{i3\theta}\rangle) \\
 & + (A_2 |S_{11}\rangle |S_{21}\rangle |S_{32}\rangle |S_{41}\rangle |\alpha e^{-i4\theta}\rangle + A_1 |S_{12}\rangle |S_{22}\rangle |S_{31}\rangle |S_{42}\rangle |\alpha e^{i4\theta}\rangle) \\
 & + (A_2 |S_{12}\rangle |S_{21}\rangle |S_{32}\rangle |S_{41}\rangle |\alpha e^{-i5\theta}\rangle + A_1 |S_{11}\rangle |S_{22}\rangle |S_{31}\rangle |S_{42}\rangle |\alpha e^{i5\theta}\rangle) \\
 & + (A_2 |S_{11}\rangle |S_{22}\rangle |S_{32}\rangle |S_{41}\rangle |\alpha e^{-i6\theta}\rangle + A_1 |S_{12}\rangle |S_{21}\rangle |S_{31}\rangle |S_{42}\rangle |\alpha e^{i6\theta}\rangle) \\
 & + (A_2 |S_{12}\rangle |S_{22}\rangle |S_{32}\rangle |S_{41}\rangle |\alpha e^{-i7\theta}\rangle + A_1 |S_{11}\rangle |S_{21}\rangle |S_{31}\rangle |S_{42}\rangle |\alpha e^{i7\theta}\rangle)].
 \end{aligned} \tag{5}$$

Performing an X-quadrature homodyne measurement [21] on the coherent state with α real, there are eight groups of measurement outcomes corresponding to eight scenarios of phase shifts ($0, \pm\theta, \pm2\theta, \pm3\theta, \pm4\theta, \pm5\theta, \pm6\theta, \pm7\theta$) denoted as Eq. (5). If zero phase shift occurs, the spatial entangled state of the four photons

$$|\psi\rangle_{1234, \text{zero}} = |H\rangle_1 |H\rangle_2 |H\rangle_3 |H\rangle_4 (A_2 |S_{11}\rangle |S_{21}\rangle |S_{31}\rangle |S_{41}\rangle + A_1 |S_{12}\rangle |S_{22}\rangle |S_{32}\rangle |S_{42}\rangle) \tag{6}$$

is created. Otherwise, nonzero phase shifts ($\pm j\theta, j = 1, 2, \dots, 7$) are obtained; a phase shift $2\phi(x, k\theta), (k = 1, 2, \dots, 7)$ operation should be performed to erase the phase difference between the two superposition terms in the scenarios of seven different nonzero phase shifts. Here $2\phi(x, k\theta) = 2\alpha \sin k\theta (x - 2\alpha \cos k\theta) \text{mod} 2\pi$ is a function of the phase shift and the eigenvalue x of the X operator. Then, some swap gates are inserted into the corresponding paths ($S_{11}, S_{12}; S_{21}, S_{22}; S_{31}, S_{32}; S_{41}, S_{42}$) to change the system state to that shown in Eq. (6). A swap gate is an important two-qubit logic gate. In terms of the basis of $\{|00\rangle, |01\rangle, |10\rangle, |11\rangle\}$, the swap gate can be represented as the following matrix:

$$\begin{bmatrix} 1 & 0 & 0 & 0 \\ 0 & 0 & 1 & 0 \\ 0 & 1 & 0 & 0 \\ 0 & 0 & 0 & 1 \end{bmatrix}. \tag{7}$$

In practice, the swap gate transformation can be yielded by the Hong-Ou-Mandel interference [36] in the Mach-Zehnder interferometer [23,37], illustrated in Fig. 2. Two beam splitters constitute a Mach-Zehnder interferometer. Additionally, the phase shifter PS π denotes the phase shift π executed on the photon passing through the line it is inserted.

Subsequently, the half-wave plates, HWP 22.5° s, are inserted into the paths $S_{11}, S_{12}, S_{31}, S_{32}$. Meanwhile, a HWP δ is inserted into the path S_{21} , and a HWP 45° is inserted into the path S_{41} . The HWP(δ) transformation function is given by $|H\rangle \rightarrow \cos 2\delta |H\rangle + \sin 2\delta |V\rangle$. So the system evolves to

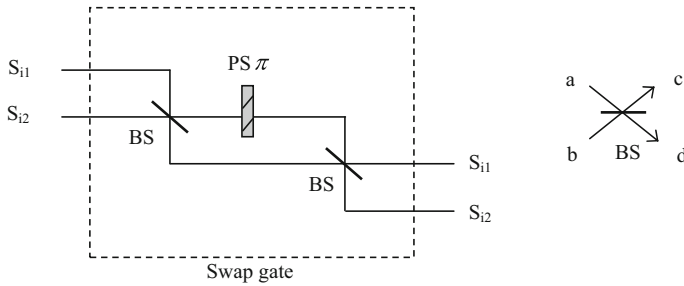


Fig. 2 Illustration plot for depicting the swap gate. The symbol $PS \pi$ denotes the phase shift π executed on the photon passing through the line it is inserted. A beam splitter has the following function between two input modes (a, b) and two output modes (c, d): $a^\dagger \rightarrow \frac{1}{\sqrt{2}}(c^\dagger + d^\dagger)$, $b^\dagger \rightarrow \frac{1}{\sqrt{2}}(d^\dagger - c^\dagger)$

$$\begin{aligned} & \frac{A_2}{2} [\cos 2\delta(|VHHV\rangle + |VHVV\rangle + |HHHV\rangle + |HHVV\rangle) \\ & + \sin 2\delta(|VVHV\rangle + |VVVV\rangle + |HVHV\rangle + |HVVV\rangle)] |S_{11}\rangle |S_{21}\rangle |S_{31}\rangle |S_{41}\rangle \\ & + \frac{A_1}{2} (|HHHH\rangle + |HHVH\rangle + |VHHH\rangle + |VHVV\rangle) |S_{12}\rangle |S_{22}\rangle |S_{32}\rangle |S_{42}\rangle. \end{aligned} \tag{8}$$

In the polarization entanglement module, four controlled-NOT (CNOT) gates are performed on the paths (S_{31}, S_{41}) , (S_{12}, S_{22}) , (S_{32}, S_{42}) and (S_{41}, S_{21}) (the photon in the former path as control photon and the photon in the latter path as target photon in each pair of paths). The CNOT gate is important in the experimental realization. Knill et al. [38] firstly proposed a probabilistic CNOT gate on two photonic qubits by using linear optical elements and postselection. The cross-Kerr nonlinearity has also been used to implement the CNOT gate [22,23,44]. After four CNOT gates, the four-photon system will evolve into

$$\begin{aligned} & \frac{A_2}{2} [\cos 2\delta(|VVHV\rangle + |VHVH\rangle + |HVHV\rangle + |HHVH\rangle) \\ & + \sin 2\delta(|VHHV\rangle + |VVVH\rangle + |HHHV\rangle + |HVVV\rangle)] |S_{11}\rangle |S_{21}\rangle |S_{31}\rangle |S_{41}\rangle \\ & + \frac{A_1}{2} (|HHHH\rangle + |HHVV\rangle + |VVHH\rangle + |VVVV\rangle) |S_{12}\rangle |S_{22}\rangle |S_{32}\rangle |S_{42}\rangle. \end{aligned} \tag{9}$$

When the photons (1,2,3) enter into the Kerr media, affected by cross-Kerr nonlinearities, the horizontal polarization mode of photons (1,2,3) via the paths $S_{11}, S_{12}, S_{21}, S_{32}$ will accumulate the phase shift θ , respectively, on the coherent state $|\alpha'\rangle$. As the consequence of the nonlinear interaction between photons and the coherent state, the state of the whole system can be expressed as

$$\begin{aligned} & \frac{A_2}{2} \{ [\cos 2\delta(|VHVH\rangle + |HVHV\rangle) + \sin 2\delta(|VHHV\rangle + |HVVV\rangle)] |\alpha'\rangle \\ & + (\cos 2\delta |HHVH\rangle + \sin 2\delta |HHHV\rangle) |\alpha' e^{i\theta}\rangle + (\cos 2\delta |VVHV\rangle \end{aligned}$$

$$\begin{aligned}
 & + \sin 2\delta |VVVH\rangle |\alpha' e^{-i\theta}\rangle |S_{11}\rangle |S_{21}\rangle |S_{31}\rangle |S_{41}\rangle \\
 & + \frac{A_1}{2} [(|HHVV\rangle + |VVHH\rangle) |\alpha'\rangle + |HHHH\rangle |\alpha' e^{i\theta}\rangle \\
 & + |VVVV\rangle |\alpha' e^{-i\theta}\rangle] |S_{12}\rangle |S_{22}\rangle |S_{32}\rangle |S_{42}\rangle.
 \end{aligned} \tag{10}$$

Perform the X-quadrature homodyne measurement on the coherent state. If zero phase shift occurs, no phase modulation is necessary. Otherwise, if nonzero phase shift is presented, three HWP45°s should be put into the paths S_{11} , S_{32} , S_{42} , respectively, and two phase shifters $PS\ 2\phi(x)$ are inserted into the circuit. After that, we can obtain the four-photon state as follows

$$\begin{aligned}
 & \frac{A_2}{\sqrt{2}} [\cos 2\delta (|HVHV\rangle + |VHVH\rangle) \\
 & + \sin 2\delta (|VHHV\rangle + |HVVH\rangle)] |S_{11}\rangle |S_{21}\rangle |S_{31}\rangle |S_{41}\rangle \\
 & + \frac{A_1}{\sqrt{2}} (|HHVV\rangle + |VVHH\rangle) |S_{12}\rangle |S_{22}\rangle |S_{32}\rangle |S_{42}\rangle.
 \end{aligned} \tag{11}$$

Before four photons leave the circuit, we let them pass through the beam splitters $BS_5 - BS_8$. According to the following rules, $a_{S_{11}}^\dagger \rightarrow \frac{1}{\sqrt{2}}(a_{S'_{11}}^\dagger + a_{S'_{12}}^\dagger)$, $a_{S_{12}}^\dagger \rightarrow \frac{1}{\sqrt{2}}(a_{S'_{12}}^\dagger - a_{S'_{11}}^\dagger)$, $a_{S_{21}}^\dagger \rightarrow \frac{1}{\sqrt{2}}(a_{S'_{21}}^\dagger - a_{S'_{22}}^\dagger)$, $a_{S_{22}}^\dagger \rightarrow \frac{1}{\sqrt{2}}(a_{S'_{22}}^\dagger + a_{S'_{21}}^\dagger)$, $a_{S_{31}}^\dagger \rightarrow \frac{1}{\sqrt{2}}(a_{S'_{31}}^\dagger - a_{S'_{32}}^\dagger)$, $a_{S_{32}}^\dagger \rightarrow \frac{1}{\sqrt{2}}(a_{S'_{32}}^\dagger + a_{S'_{31}}^\dagger)$, $a_{S_{41}}^\dagger \rightarrow \frac{1}{\sqrt{2}}(a_{S'_{41}}^\dagger + a_{S'_{42}}^\dagger)$, and $a_{S_{42}}^\dagger \rightarrow \frac{1}{\sqrt{2}}(a_{S'_{42}}^\dagger - a_{S'_{41}}^\dagger)$, at the output ports, the state of four photons expressed as Eq. (11) is transformed to

$$\begin{aligned}
 & \frac{1}{4\sqrt{2}} \{ [A_2 \cos 2\delta (|HVHV\rangle + |VHVH\rangle) + A_2 \sin 2\delta (|VHHV\rangle + |HVVH\rangle) \\
 & + A_1 (|HHVV\rangle + |VVHH\rangle)] (|S'_{11}\rangle |S'_{21}\rangle |S'_{31}\rangle |S'_{41}\rangle - |S'_{11}\rangle |S'_{21}\rangle |S'_{32}\rangle |S'_{42}\rangle \\
 & - |S'_{11}\rangle |S'_{22}\rangle |S'_{31}\rangle |S'_{42}\rangle + |S'_{11}\rangle |S'_{22}\rangle |S'_{32}\rangle |S'_{41}\rangle + |S'_{12}\rangle |S'_{21}\rangle |S'_{31}\rangle |S'_{42}\rangle \\
 & - |S'_{12}\rangle |S'_{21}\rangle |S'_{32}\rangle |S'_{41}\rangle - |S'_{12}\rangle |S'_{22}\rangle |S'_{31}\rangle |S'_{41}\rangle + |S'_{12}\rangle |S'_{22}\rangle |S'_{32}\rangle |S'_{42}\rangle) \\
 & + [A_2 \cos 2\delta (|HVHV\rangle + |VHVH\rangle) + A_2 \sin 2\delta (|VHHV\rangle + |HVVH\rangle) \\
 & - A_1 (|HHVV\rangle + |VVHH\rangle)] (|S'_{11}\rangle |S'_{21}\rangle |S'_{31}\rangle |S'_{42}\rangle - |S'_{11}\rangle |S'_{21}\rangle |S'_{32}\rangle |S'_{41}\rangle \\
 & - |S'_{11}\rangle |S'_{22}\rangle |S'_{31}\rangle |S'_{41}\rangle + |S'_{11}\rangle |S'_{22}\rangle |S'_{32}\rangle |S'_{42}\rangle + |S'_{12}\rangle |S'_{21}\rangle |S'_{31}\rangle |S'_{41}\rangle \\
 & - |S'_{12}\rangle |S'_{21}\rangle |S'_{32}\rangle |S'_{42}\rangle - |S'_{12}\rangle |S'_{22}\rangle |S'_{31}\rangle |S'_{42}\rangle + |S'_{12}\rangle |S'_{22}\rangle |S'_{32}\rangle |S'_{41}\rangle) \}.
 \end{aligned} \tag{12}$$

From the above equation, we can see that by detecting the outputs of the four photons, if the state $A_2 \cos 2\delta (|HVHV\rangle + |VHVH\rangle) + A_2 \sin 2\delta (|VHHV\rangle + |HVVH\rangle) - A_1 (|HHVV\rangle + |VVHH\rangle)$ is obtained, two HWPs are employed to be performed $\sigma_z \sigma_z$ on the photons (1, 2) or the photons (3, 4). Finally, we obtain

$$\begin{aligned}
 & \frac{A_2 \cos 2\delta}{\sqrt{2}} (|HVHV\rangle + |VHVH\rangle) + \frac{A_2 \sin 2\delta}{\sqrt{2}} (|VHHV\rangle + |HVVH\rangle) \\
 & + \frac{A_1}{\sqrt{2}} (|HHVV\rangle + |VVHH\rangle).
 \end{aligned} \tag{13}$$

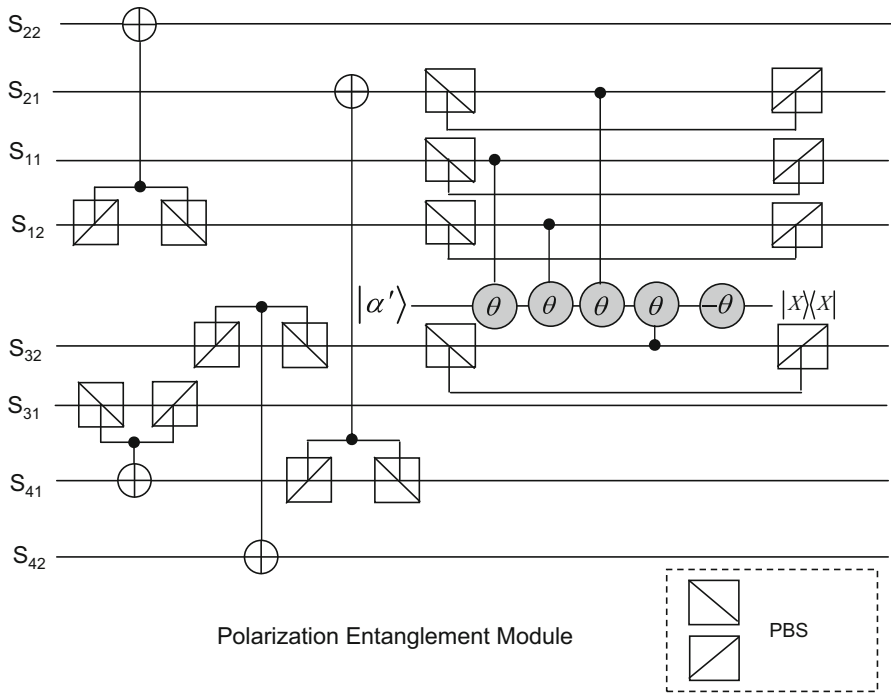


Fig. 3 Illustration plot for depicting a polarization entanglement module. The *left part* represents the photonic CNOT gates assisted by cross-Kerr nonlinearities, which can be realized in Refs. [22,23,44]. The polarization beam splitters (PBS) reflect the vertical polarization $|V\rangle$ mode and transmit the horizontal polarization $|H\rangle$ mode. After the CNOT gates, the photons (1,2,3) pass through the Kerr medium. Influenced by cross-Kerr nonlinearities, the photons (1,2,3) in the horizontal polarization state enable the coherent state $|\alpha\rangle$ to pick up the phase shift θ , respectively, while the phase shifter $-\theta$ is applied to generate the minus phase shift

By modulating the coefficients A_1, A_2 and δ as $A_1 = \sqrt{\frac{2}{3}}\beta, A_2 \sin 2\delta = -\frac{\alpha}{\sqrt{2}} - \frac{\beta}{\sqrt{6}}$ and $A_2 \cos 2\delta = \frac{\alpha}{\sqrt{2}} - \frac{\beta}{\sqrt{6}}$, we can obtain

$$\begin{aligned}
 |\psi\rangle_L &= \alpha|0\rangle_L + \beta|1\rangle_L = \frac{\alpha}{2}(|HV\rangle - |VH\rangle)(|HV\rangle - |VH\rangle) \\
 &+ \frac{\beta}{2\sqrt{3}}(2|VVHH\rangle + 2|HHVV\rangle - |VHVH\rangle - |VHHV\rangle \\
 &- |HVHV\rangle - |HVVH\rangle)|_{1234}.
 \end{aligned}
 \tag{14}$$

That is, the generation of four-photon polarization-entangled decoherence-free state is achieved. Compared with the previous protocol in Ref. [33], which can be iterated to get a good success probability, the present one is the first nearly deterministic scheme to prepare the four-photon polarization-entangled decoherence-free state based on cross-Kerr nonlinearities (Fig. 3).

3 Discussion and conclusion

So far, we have shown an alternative scheme for photonic qubits in generating an entangled decoherence-free state. We now give a brief discussion about the experimental feasibility of protocol with the current experimental technology. First of all, the cross-Kerr nonlinearities are exploited in the spatial entanglement process and the polarization entanglement module. Although a lot of works have been studied in the area of cross-Kerr nonlinearities, we should acknowledge that it is still a quite controversial concept to have a clean cross-Kerr nonlinearity in the optical single-photon regime with present science and technology. What is worse, the natural cross-Kerr nonlinearities are extremely small and unsuitable for single-photon interaction. Hence, various physics systems or artificial media such as negative index metamaterials [39], a superconducting artificial atom [40] and three-dimensional circuit quantum electrodynamic architecture [41, 42] are investigated to achieve larger strength of cross-Kerr nonlinearities. Second, the experiment feasibility of the present protocol also depends on the veracity of the X-quadrature homodyne measurement. Without considering other conditions, the error chiefly comes from the overlap of adjacent curves because of the fact that the coherent states of the probe beam with different phase shifts are not completely orthogonal. In fact, it is only one type of detection error in homodyne; other errors, such as the noises in detection, the reduced fidelity to the process in Eq. (4) due to multi-mode effect and decoherence, etc., also exist in a realistic implementation. Exploiting the appropriate measurement methods, the disadvantageous influence can be overcome or alleviated and the error probability will be decreased. In 2010, Wittmann et al. [43] investigated quantum measurement strategies capable of discriminating two coherent states using a homodyne detector and a photon number resolving (PNR) detector. In order to lower the error probability, the postselection strategy is applied to the measurement data of homodyne detector as well as a PNR detector. They indicated that the performance of the new displacement-controlled PNR is better than homodyne receiver. Finally, one can see that four CNOT gates are performed in the polarization entanglement module. Employing weak cross-Kerr nonlinearities, a nearly deterministic CNOT gate was put forward by Nemoto and Munro [22] with one auxiliary photon. At the price of halving the construction probability, Lin and Li [23] proposed a CNOT gate without the ancilla photon. Motivated by these schemes, Xiu et al. [44] presented a scheme for constructing the nearly deterministic CNOT gate, where the auxiliary photon is not necessary. However, these methods are at the best, nearly deterministic, so our scheme could be nearly deterministic.

To summarize, we have proposed the detailed generation circuit of the four-photon polarization-entangled decoherence-free state with the assistance of the cross-Kerr nonlinearities. In our protocol, combined with some swap gates and simple linear optical elements, two main processes including the four-photon spatial entanglement process and the four-photon polarization entanglement process are applied. This protocol can be implemented nearly deterministically in principle. By virtue of the availability of optical elements and techniques involved, we hope the generation scheme is feasible and it will stimulate investigations on the applications of four-qubit decoherence-free states based on optics.

Acknowledgements This work was supported by the National Natural Science Foundation of China under Grant Nos. 11475054, 11371005, Hebei Natural Science Foundation of China under Grant No. A2016205145 and the Education Department of Hebei Province Natural Science Foundation under Grant No. QN2017089.

References

- Horodecki, R., Horodecki, P., Horodecki, M., Horodecki, K.: Quantum entanglement. *Rev. Mod. Phys.* **81**, 865–942 (2009)
- Yan, F.L., Gao, T., Chitambar, E.: Two local observables are sufficient to characterize maximally entangled states of N qubits. *Phys. Rev. A* **83**, 022319 (2011)
- Gao, T., Yan, F.L., van Enk, S.J.: Permutationally invariant part of a density matrix and nonseparability of N -qubit states. *Phys. Rev. Lett.* **112**, 180501 (2014)
- Terhal, B.M., Burkard, G.: Fault-tolerant quantum computation for local non-Markovian noise. *Phys. Rev. A* **71**, 012336 (2005)
- Aharonov, D., Kitaev, A., Preskill, J.: Fault-tolerant quantum computation with long-range correlated noise. *Phys. Rev. Lett.* **96**, 050504 (2006)
- Viola, L., Knill, E., Lloyd, S.: Dynamical decoupling of open quantum systems. *Phys. Rev. Lett.* **82**, 2417–2421 (1999)
- Xu, G.F., Long, G.L.: Protecting geometric gates by dynamical decoupling. *Phys. Rev. A* **90**, 022323 (2014)
- Bennett, C.H., Bernstein, H.J., Popescu, S., Schumacher, B.: Concentrating partial entanglement by local operations. *Phys. Rev. A* **53**, 2046–2052 (1996)
- Zhao, Z., Yang, T., Chen, Y.A., Zhang, A.N., Pan, J.W.: Experimental realization of entanglement concentration and a quantum repeater. *Phys. Rev. Lett.* **90**, 207901 (2003)
- Deng, F.G.: Optimal nonlocal multipartite entanglement concentration based on projection measurements. *Phys. Rev. A* **85**, 022311 (2012)
- Sheng, Y.B., Zhou, L., Zhao, S.M.: Efficient two-step entanglement concentration for arbitrary W states. *Phys. Rev. A* **85**, 042302 (2012)
- Duan, L.M., Guo, G.C.: Preserving coherence in quantum computation by pairing quantum bits. *Phys. Rev. Lett.* **79**, 1953–1956 (1997)
- Zanardi, P., Rasetti, M.: Noiseless quantum codes. *Phys. Rev. Lett.* **79**, 3306–3309 (1997)
- Kempe, J., Bacon, D., Lidar, D.A., Whaley, K.B.: Theory of decoherence-free fault-tolerant universal quantum computation. *Phys. Rev. A* **63**, 042307 (2001)
- Altepeter, J.B., Hadley, P.G., Wendelken, S.M., Berglund, A.J., Kwiat, P.G.: Experimental investigation of a two-qubit decoherence-free subspace. *Phys. Rev. Lett.* **92**, 147901 (2004)
- Bourennane, M., Eibl, M., Gaertner, S., Kurtsiefer, C., Cabello, A., Weinfurter, H.: Decoherence-free quantum information processing with four-photon entangled states. *Phys. Rev. Lett.* **92**, 107901 (2004)
- Zou, X.B., Shu, J., Guo, G.C.: Simple scheme for generating four-photon polarization-entangled decoherence-free states using spontaneous parametric down-conversions. *Phys. Rev. A* **73**, 054301 (2006)
- Gong, Y.X., Zou, X.B., Niu, X.L., Li, J., Huang, Y.F., Guo, G.C.: Generation of arbitrary four-photon polarization-entangled decoherence-free states. *Phys. Rev. A* **77**, 042317 (2008)
- Wang, H.F., Zhang, S., Zhu, A.D., Yi, X.X., Yeon, K.H.: Local conversion of four Einstein–Podolsky–Rosen photon pairs into four-photon polarization-entangled decoherence-free states with non-photon-number-resolving detectors. *Opt. Express* **19**, 25433–25440 (2011)
- Zhou, Y.S., Li, X., Deng, Y., Li, H.R., Luo, M.X.: Generation of hybrid four-qubit entangled decoherence-free states assisted by the cavity-QED system. *Opt. Commun.* **366**, 397–403 (2016)
- Barrett, S.D., Kok, P., Nemoto, K., Beausoleil, R.G., Munro, W.J., Spiller, T.P.: Symmetry analyzer for nondestructive Bell-state detection using weak nonlinearities. *Phys. Rev. A* **71**, 060302 (2005)
- Nemoto, K., Munro, W.J.: Nearly deterministic linear optical controlled-NOT gate. *Phys. Rev. Lett.* **93**, 250502 (2004)
- Lin, Q., Li, J.: Quantum control gates with weak cross-Kerr nonlinearity. *Phys. Rev. A* **79**, 022301 (2009)
- Lin, Q., He, B.: Single-photon logic gates using minimal resources. *Phys. Rev. A* **80**, 042310 (2009)

25. Sheng, Y.B., Zhou, L.: Deterministic entanglement distillation for secure double-server blind quantum computation. *Sci. Rep.* **5**, 7815 (2015)
26. Ding, D., Yan, F.L., Gao, T.: Preparation of km-photon concatenated Greenberger–Horne–Zeilinger states for observing distinctive quantum effects at macroscopic scales. *J. Opt. Soc. Am. B* **30**, 3075–3078 (2013)
27. Sheng, Y.B., Zhou, L.: Two-step complete polarization logic Bell-state analysis. *Sci. Rep.* **5**, 13453 (2015)
28. He, Y.Q., Ding, D., Yan, F.L., Gao, T.: Exploration of multiphoton entangled states by using weak nonlinearities. *Sci. Rep.* **6**, 19116 (2016)
29. He, Y.Q., Ding, D., Yan, F.L., Gao, T.: Exploration of photon-number entangled states using weak nonlinearities. *Opt. Express* **23**, 21671 (2015)
30. Dong, L., Wang, J.X., Li, Q.Y., Shen, H.Z., Dong, H.K., Xiu, X.M.: Nearly deterministic preparation of the perfect W state with weak cross-Kerr nonlinearities. *Phys. Rev. A* **93**, 012308 (2016)
31. Lin, Q., He, B.: Highly efficient processing of multi-photon states. *Sci. Rep.* **5**, 12792 (2015)
32. Dong, L., Wang, J.X., Li, Q.Y., Shen, H.Z., Dong, H.K., Xiu, X.M., Gao, Y.J.: Single logical qubit information encoding scheme with the minimal optical decoherence-free subsystem. *Opt. Lett.* **41**, 1030–1033 (2016)
33. Xia, Y., Lu, M., Song, J., Lu, P.M., Song, H.S.: Effective protocol for preparation of four-photon polarization-entangled decoherence-free states with cross-Kerr nonlinearity. *J. Opt. Soc. Am. B* **30**, 421–427 (2013)
34. Chuang, I.L., Yamamoto, Y.: Simple quantum computer. *Phys. Rev. A* **52**, 3489–3496 (1995)
35. Munro, W.J., Nemoto, K., Beausoleil, R.G., Spiller, T.P.: High-efficiency quantum-nondemolition single-photon-number-resolving detector. *Phys. Rev. A* **71**, 033819 (2005)
36. Hong, C.K., Ou, Z.Y., Mandel, L.: Measurement of subpicosecond time intervals between two photons by interference. *Phys. Rev. Lett.* **59**, 2044–2046 (1987)
37. Milburn, G.J.: Quantum optical Fredkin gate. *Phys. Rev. Lett.* **62**, 2124–2127 (1989)
38. Knill, E., Laflamme, R., Milburn, G.J.: A scheme for efficient quantum computation with linear optics. *Nature* **409**, 46–52 (2001)
39. Siomau, M., Kamli, A.A., Moiseev, S.A., Sanders, B.C.: Entanglement creation with negative index metamaterials. *Phys. Rev. A* **85**, 050303 (2012)
40. Hoi, I.C., Kockum, A.F., Palomaki, T., Stace, T.M., Fan, B., Tornberg, L., Sathyamoorthy, S.R., Johansson, G., Delsing, P., Wilson, C.M.: Giant cross-Kerr effect for propagating microwaves induced by an artificial atom. *Phys. Rev. Lett.* **111**, 053601 (2013)
41. Paik, H., Schuster, D.I., Bishop, L.S., Kirchmair, G., Catelani, G., Sears, A.P., Johnson, B.R., Reagor, M.J., Frunzio, L., Glazman, L.I., Girvin, S.M., Devoret, M.H., Schoelkopf, R.J.: Observation of high coherence in Josephson junction qubits measured in a three-dimensional circuit QED architecture. *Phys. Rev. Lett.* **107**, 240501 (2011)
42. Kirchmair, G., Vlastakis, B., Leghtas, Z., Nigg, S.E., Paik, H., Ginossar, E., Mirrahimi, M., Frunzio, L., Girvin, S.M., Schoelkopf, R.J.: Observation of quantum state collapse and revival due to the single-photon Kerr effect. *Nature* **495**, 205–209 (2013)
43. Wittmann, C., Andersen, U.L., Takeoka, M., Leuchs, G.: Discrimination of binary coherent states using a homodyne detector and a photon number resolving detector. *Phys. Rev. A* **81**, 062338 (2010)
44. Xiu, X.M., Dong, L., Gao, Y.J., Yi, X.X.: Nearly deterministic controlled-NOT gate with weak cross-Kerr nonlinearities. *Quantum Inf. Comput.* **12**, 0159–0170 (2012)